Effects of integrin-mediated cell adhesion on plasma membrane lipid raft components and signaling

Andrés Norambuena[a] and Martin A. Schwartz[a,b,*]
[a]Robert M. Berne Cardiovascular Research Center and [b]Departments of Microbiology, Cell Biology, and Biomedical Engineering; Mellon Urological Cancer Research Institute, University of Virginia, Charlottesville, VA 22908

ABSTRACT **Anchorage dependence of cell growth, which is mediated by multiple integrin-regulated signaling pathways, is a key defense against cancer metastasis. Detachment of cells from the extracellular matrix triggers caveolin-1–dependent internalization of lipid raft components, which mediates suppression of Rho GTPases, Erk, and phosphatidylinositol 3-kinase in suspended cells. Elevation of cyclic adenosine monophosphate (cAMP) following cell detachment is also implicated in termination of growth signaling in suspended cells. Studies of integrins and lipid rafts, however, examined mainly ganglioside GM1 and glycosylphosphatidylinositol-linked proteins as lipid raft markers. In this study, we examine a wider range of lipid raft components. Whereas many raft components internalized with GM1 following cell detachment, flotillin2, connexin43, and $G\alpha_s$ remained in the plasma membrane. Loss of cell adhesion caused movement of many components from the lipid raft to the nonraft fractions on sucrose gradients, although flotillin2, connexin43, and H-Ras were resistant. $G\alpha_s$ lost its raft association, concomitant with cAMP production. Modification of the lipid tail of $G\alpha_s$ to increase its association with ordered domains blocked the detachment-induced increase in cAMP. These data define the effects of that integrin-mediated adhesion on the localization and behavior of a variety of lipid raft components and reveal the mechanism of the previously described elevation of cAMP after cell detachment.**

Monitoring Editor
Josephine Clare Adams
University of Bristol

Received: Apr 25, 2011
Revised: Jul 7, 2011
Accepted: Jul 18, 2011

INTRODUCTION

Normal cells require anchorage to an extracellular matrix (ECM) for growth and survival due to the requirement for integrin-dependent signals in these processes. Integrin-mediated adhesion modulates signaling events downstream of tyrosine kinases and G protein–coupled receptors to control many signaling pathways. Loss of this requirement in cancer cells leads to anchorage-independent growth, which closely correlates with tumorigenicity and metastasis in vivo (Schwartz, 1997). As even nonmetastatic cancers can shed large numbers of cells into the circulation (Bockhorn *et al.*, 2007), their failure to survive and grow in inappropriate environments is thought to be an important defense against metastasis. Previous studies implicated cyclic adenosine monophosphate (cAMP) and protein kinase A (PKA) in terminating growth signals upon cell detachment (Howe and Juliano, 2000). The mechanism by which adenylyl cyclase (AC) is activated under these conditions has not been elucidated, however.

Eukaryotic cell membranes contain several different types of liquid-ordered domains with high concentrations of cholesterol and saturated lipids, often termed "lipid rafts." These domains are also enriched in sphingolipids and glycosylphosphatidylinositol (GPI)-linked and other lipid-linked proteins (Brown and London, 1998; Simons and Toomre, 2000). The current consensus is that lipid rafts are dynamic structures on dimensional scales of 5–200 nm, the properties of which are strongly influenced by their protein content (Lingwood and Simons, 2010). These domains can modulate signaling pathways in diverse biological processes such as cell division,

This article was published online ahead of print in MBoC in Press (http://www.molbiolcell.org/cgi/doi/10.1091/mbc.E11-04-0361) on July 27, 2011.

*Present address: Departments of Medicine and Cell Biology, Yale University School of Medicine, New Haven, CT 06511.

Address correspondence to: Martin A. Schwartz (mas5bm@virginia.edu).

Abbreviations used: AC, adenylyl cyclase; cAMP, cyclic adenosine monophosphate; Cav1, caveolin-1; CTxB, cholera toxin subunit B; DRM, detergent-resistant membranes; ECM, extracellular matrix; FRS2, fibroblast growth factor receptor substrate 2; GFP, green fluorescent protein; GPI, glycosylphosphatidylinositol; MEF, murine embryonic fibroblast; PBS, phosphate-buffered saline; PI, phosphatidylinositol; PKA, protein kinase A; PM, plasma membrane; WT, wild type.

apoptosis, adhesion, and migration (Brown and London, 1998; Simons and Toomre, 2000). Lipid rafts modulate spatial targeting of GTPases required for cell spreading and migration (Manes *et al.*, 1999; del Pozo *et al.*, 2004). Interestingly, adhesion sites have high membrane order, suggesting a raft-like composition (Gaus *et al.*, 2006).

In anchorage-dependent cells, loss of integrin-mediated adhesion stimulates caveolin-1 (Cav1)-dependent internalization of rafts from the plasma membrane (PM) and transport to the recycling endosomes, leading to dramatically decreased PM order (del Pozo *et al.*, 2004, 2005; Gaus *et al.*, 2006; Balasubramanian *et al.*, 2007). The resultant alteration in PM organization down-regulates Rac1, Erk, and phosphatidylinositol (PI) 3-kinase–dependent pathways. Replating cells on fibronectin or other ECM proteins stimulates return of raft components to the PM, which restores anchorage-dependent signaling. This exocytosis pathway requires activation of ARF6, which stimulates exit of raft components from the recycling endosomes, and activation of RalA, which, through its effector the exocyst, mediates vesicle docking at the PM during exocytosis (Balasubramanian *et al.*, 2007, 2010)

The studies just mentioned examined mainly GPI-linked proteins and ganglioside GM1 as raft markers. Many proteins, however, partition into lipid rafts, and their fate has not been examined. In particular, the effects of raft endocytosis on many signaling proteins are unknown. We therefore examined multiple raft and nonraft PM components, including both structural and signaling proteins, after cell detachment from the ECM. Our results showed, first, that loss of cell adhesion alters the localization and raft partitioning of many but not all raft components. Second, we found that these events control $G\alpha_s$–lipid raft interaction to increase cAMP levels. Our results therefore reveal the mechanism by which loss of cell adhesion activates PKA.

RESULTS

Loss of cell adhesion triggers internalization of many but not all raft components

We previously found that cell detachment triggers caveolin-dependent internalization of GM1, cholesterol, and GPI-linked proteins; internalization required tyrosine phosphorylation on Cav1 (Tyr14), dynamin II, and the actin cytoskeleton (del Pozo *et al.*, 2005; Balasubramanian *et al.*, 2007). To test the fate of additional raft-associated lipids and proteins following cell detachment, we compared their localization with GM1 in NIH 3T3 cells. For these experiments, serum-starved, adherent cells were surface stained for GM1 at 4°C and then warmed to 37°C, detached, and examined at subsequent times. Immediately after detachment (0–3 min), GM1 strongly colocalized at the PM with green fluorescent protein (GFP)-tagged versions of H-Ras, K-Ras, Src, Fyn(T), integrin α5, and RalA (Figure 1, A–F; cell edge vs. cell center quantified in H and summarized in Table 1). After incubation for 90 min, GM1 was internalized and accumulated in RE as expected. The other markers also showed substantial relocalization to the RE, although GFP-H-Ras and GFP-α5 did so less efficiently, with a larger fraction remaining at the PM (Figure 1, A and E, quantifications in H and summarized in Table 1). Loss of cell adhesion also induced the internalization of GFP-GPI (Figure 1, G and H). GFP-flotillin2, YFP-Na+/K+ ATPase (α subunit), and GFP-H-Ras^{G12V} behaved differently, however; these rafts markers stayed largely at the cell surface (Figure 2, A–C, quantifications in D and summarized in Table 1), whereas GM1 in the same cells internalized normally.

To confirm these results, we fractionated cells by using low-speed centrifugation that efficiently sediments PMs but not recycling endosomes (Supplemental Figure 1A). Western blot analysis of endogenous raft markers correlated well with localization of GFP fusions. Cav1, RalA, Rac1, H-Ras, c-Src, and Fyn decreased in the PM–enriched fractions after cell detachment, whereas H-Ras^{V12}, flotillin2, and connexin43 showed only small changes (Supplemental Figure 1, B and C, and summarized in Table 1). Examination of additional raft markers showed that fibroblast growth factor receptor substrate 2 (FRS2) was strongly decreased in the low speed, PM-enriched fraction, whereas platelet-derived growth factor receptor β (PDGFRβ) decreased by a smaller amount. Thus, cell adhesion controls PM localization of many but not all raft components.

Our previous work showed that GM1 internalization required Cav1 (del Pozo *et al.*, 2005); thus, we examined its localization during endocytosis of the raft markers. In adherent NIH 3T3 cells, many of the raft marker cells moderately but significantly colocalized with Cav1 at cell edges (e.g., GFP–GPI in Figure 3, A and B; see also Supplemental Figure 4). Colocalization increased immediately after detachment and then further increased with time in suspension (Figure 3, A and B). By contrast, GFP–flotillin2 showed little colocalization with caveolin-1 at any time, consistent with its failure to internalize (Figure 3B and Supplemental Figure 4). We next confirmed Cav1 dependence by examining the raft markers in wild type (WT) versus Cav1$^{-/-}$ murine embryonic fibroblasts (MEFs) (del Pozo *et al.*, 2004). Cav1$^{-/-}$ MEFs internalized neither GM1 (del Pozo *et al.*, 2005) nor any of the GFP-tagged constructs analyzed, whereas WT MEFs behaved similarly to 3T3s (Figure 3C). Re-expression of flag-tagged Cav1 restored their internalization (Figure 3C). Thus, Cav1 is required for detachment-induced internalization of all of the lipid raft proteins that we examined.

Effects of cell adhesion on raft marker association with lipid rafts

We previously found that detachment-induced internalization of lipid raft components led to a decrease in lipid order at the PM (Gaus *et al.*, 2006). We therefore addressed whether the lipid raft markers examined here altered their partitioning into the low density, raft fraction on sucrose gradients. Whole-cell lysates in Triton X-100 (either 0.25 or 1%, as indicated) from adherent or suspended cells were separated on sucrose gradients, and endogenous components were analyzed by Western blotting. GM1 in the low-density fraction decreased slightly (15 ± 4%) immediately after detachment (0–3 min), then further decreased by 40 ± 8% after 90 min (Table 1 and Supplemental Figure 2). Cav1, RalA, and Rac shifted almost completely from the low- to the high-density fractions. Src and Fyn had lower initial association with the low-density fraction, which was completely lost following cell detachment. By contrast, H-Ras, flotillin2, and connexin43 showed little change (Table 1 and Supplemental Figure 2).

Heterotrimeric G proteins are strongly localized to lipid rafts, and this localization influences their activation and signaling (Patel *et al.*, 2008). To determine whether detachment-induced changes in membrane properties affected these proteins, we examined the behavior of $G\alpha_s$. GFP-$G\alpha_s$ remained entirely in the PM following cell detachment (Figure 4A). Sucrose gradients, however, showed a complete shift from the low- to the high-density fractions (Figure 4B). Taken together, these data indicate that lipid raft proteins can exhibit several different behaviors in which efficiency of internalization and localization to lipid raft domains as defined by sucrose gradients are controlled independently. Although this idea was not explored in detail, we note that affinity for cholesterol may determine this selectivity; when total cholesterol was reduced by treating cells with cyclodextrin, flotillin2 was highly resistant compared with caveolin-1 and Src (Supplemental Figure 3).

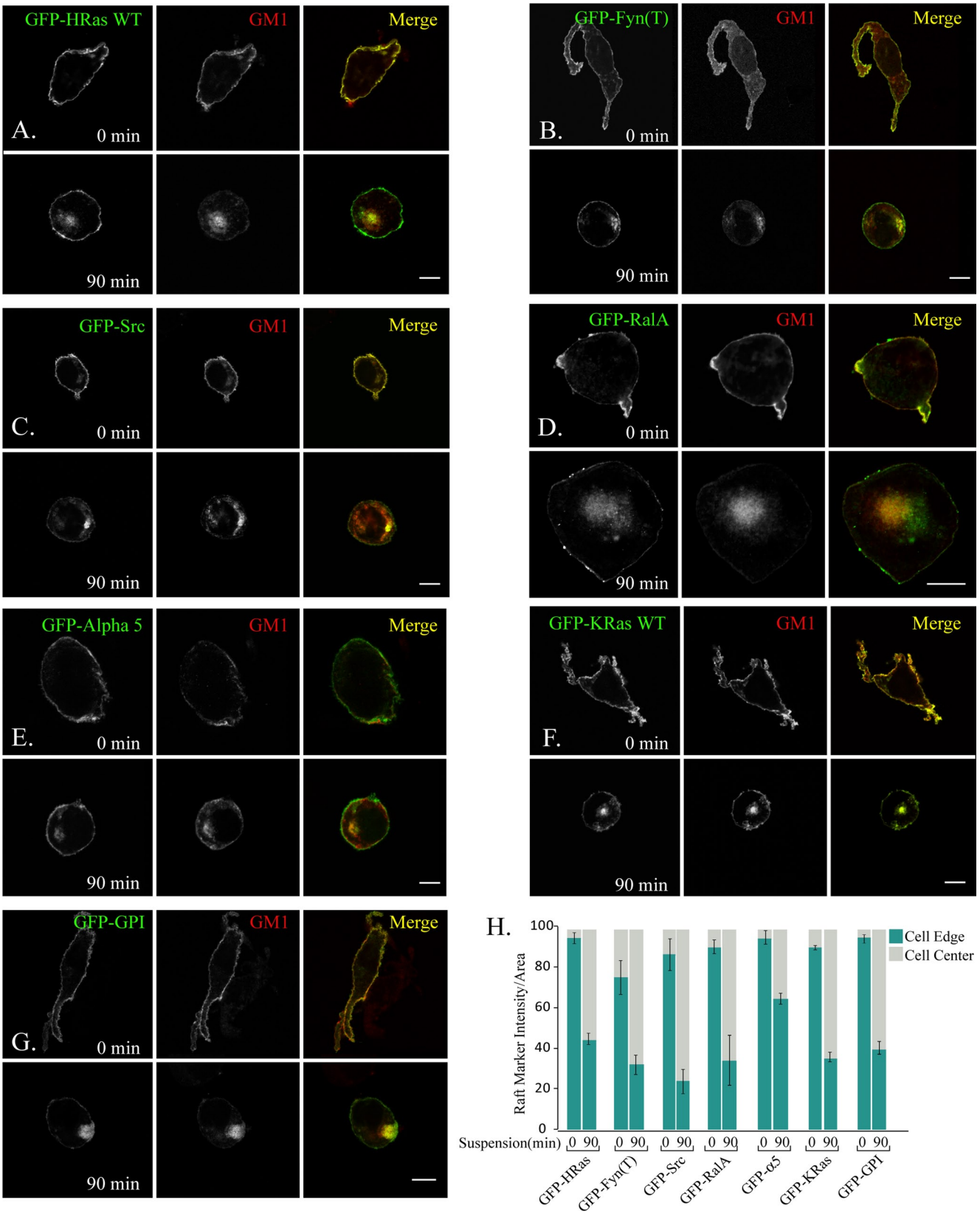

FIGURE 1: Cell detachment induces internalization of raft proteins. (A–G) Stably adherent NIH 3T3 cells transfected with different GFP constructs were surface-labeled with CTxB-Alexa 594 on ice at 4°C (GM1-CTxB), warmed to 37°C, and then detached and kept in suspension. At the indicated times (minutes), cells were fixed and processed for microscopy. Cells were stained for the raft marker GM1 as a positive control. (H) Fluorescence intensity (as a percentage of total intensity) was determined at the cell edge and the cell center. Values are mean ± SE, n = 15 cells; two independent experiments gave similar results. Bar, 10 μM.

Marker	Loss of lipid rafts association after 0- to 5-min suspension	Internalization after 90- min suspension
Caveolin-1	++	++
Flotillin 2	—	—
Flotillin 2–GFP	N.D.	—
Fyn	+++	++
Fyn(T)–GFP	N.D.	++
Src	+++	++
Src–GFP	N.D.	++
GFP–GPI	++	++
GM1	++	++
Gαs	+++	N.D.
Gαs–GFP	+++	—
RalA	+	++
RalA–GFP	N.D.	++
Rac	+	++ (PM dissociation)
Integrin α5−GFP	#	+
Na/K ATPase α1−YFP	#	—
GFP–$HRas^{G12V}$	N.D.	–
GFP–$HRas^{WT}$	++	++
HRas	+	++
GFP–$KRas^{WT}$	N.D.	++
Connexin43	—	N.D.
PDGFR	#	+
FRS2	#	+

Second column: Lipid raft markers were analyzed for partitioning into the raft fractions by flotation on sucrose gradients before and after detachment. Movement out of the low-density fraction after detachment is denoted by +. Third column: Subcellular distributions were determined from fluorescence (GFP-tagged markers and CTxB-A596) or by isolating PM-enriched fractions (endogenously expressed markers). Internalization after detachment is denoted by +.

+++: >50%; ++: ≈50%; +: <50%; —: no change; N.D: Non determined; #: low association to lipid rafts in stably adherent cell.

TABLE 1: Summary of changes in raft markers in adherent versus suspended cells.

Effects on $G\alpha_s$ signaling

To explore consequences for cell signaling, we focused on $G\alpha_s$, which mediates activation of AC to produce cAMP (Beavo and Brunton, 2002). Interestingly, the efficiency of coupling between $G\alpha_s$ and G protein—coupled receptors is cholesterol-dependent, such that depletion of cholesterol increases cAMP production (Pontier *et al.*, 2008; Allen *et al.*, 2009). Elevated cAMP is also implicated in inhibition of Erk and cell-cycle blockade following cell detachment (Howe and Juliano, 2000). We therefore investigated whether effects of adhesion on lipid rafts mediates the activation of this pathway following cell detachment. Serum-starved NIH 3T3 cells, either adherent or suspended, were stimulated with the β adrenergic receptor agonist isoproterenol over a range of concentrations. Detachment increased basal cAMP (27.29 ± 4.5 vs. 60.64 ± 6.8 pmol) as well the maximal response in the presence of isoproterenol (91.62 ± 4.37 vs. 135.6 ± 5.7 pmol). This increase in cAMP was independent of the methodology used for cell detachment when comparing enzymatic versus mechanical procedures (Supplemental Figure 5). The potency of the agonist, however, was unchanged ($LogEC_{50}$ –6.56 ± 0.211 and –6.82 ± 0.24 in adherent vs. suspension, respectively). This effect is virtually identical to what was reported for cells treated with cyclodextrin (Pontier *et al.*, 2008; Allen *et al.*, 2009).

To identify the adhesion-sensitive site within the $\beta_2AR/G_s/AC$ cascade, we activated different components within this pathway. First, cells were treated with cholera toxin, which activates G_s through irreversible ADP-ribosylation (De Haan and Hirst, 2004). Cholera toxin substantially reduced but did not completely abolish the effect of cell adhesion on cAMP levels (Figure 4D). Adhesion may therefore control both $G\alpha_s$ activation and coupling to AC. We also stimulated cells with forskolin, which acts directly on AC. The combined effects of detachment and forskolin were also additive (Figure 4E). The effects of forskolin are known to be enhanced by $G\alpha_s$ activation (Alousi *et al.*, 1991); thus these effects are consistent with enhanced $G\alpha_s$ activation and coupling.

To test whether these effects required lipid raft internalization, we repeated these experiments in WT versus $Cav1^{-/-}$ MEFs. We found that detachment of WT MEFs triggered a similar increase in cAMP levels; however, no such effect was observed in $Cav1^{-/-}$ cells. Re-expression of flag-tagged Cav1 restored the adhesion-dependent increases in cAMP (Figure 4E). Given the known ability of cholesterol depletion to activate cAMP signaling (Pontier *et al.*, 2008; Allen *et al.*, 2009), these data suggest that internalization of lipid raft components and decreased cholesterol in the PM may mediate detachment-induced cAMP production through effects on the partitioning of $G\alpha_s$ between ordered and disordered domains.

To further test this hypothesis, we considered that $G\alpha_s$ partitioning between fluid and liquid ordered domains is determined by its lipid modification. $G\alpha_s$ has a single N-terminal palmitoyl group, which mediates its association with ordered domains, whereas $G\alpha_q$ contains two and associates more strongly with ordered domains (Marrari *et al.*, 2007). To enhance lipid raft association, we therefore constructed a $G\alpha_s$ mutant that contained the N terminus of $G\alpha_q$ (G_{qs}). These proteins were tagged with GFP (Figure 5A). Both proteins expressed at equal levels (Figure 5B) and localized to the PM (Figure 5C). Analysis of sucrose gradients confirmed that GFP-G_{qs} associated more strongly with the low density, lipid raft fractions and was resistant to the cell detachment–induced movement into the nonraft fraction (compare Figure 5D with Figure 4A). Overexpression of these proteins had no effect on the partitioning of endogenous $G\alpha_s$ (Supplemental Figure 6). Whereas overexpression of GFP-G_s increased basal cAMP and enhanced detachment-induced cAMP production relative to mock-transfected cells, GFP-G_{qs} elevated basal cAMP but failed to magnify the effect of cell detachment. GFP-G_{qs} also gave similar responses to isoproterenol compared with WT GFP-G_s, indicating that it is fully functional. Thus, reducing the movement of $G\alpha_s$ into nonraft domains specifically prevented the detachment-induced increase in cAMP.

DISCUSSION

The goal of this study was to explore the consequences of lipid raft internalization for a wider range of raft components, focusing on signaling proteins. We found that cell detachment triggered movement of many but not all raft components from the PM to the recycling endosomes. Both Ras family GTPases and Src family kinases are substantially internalized, although with somewhat different

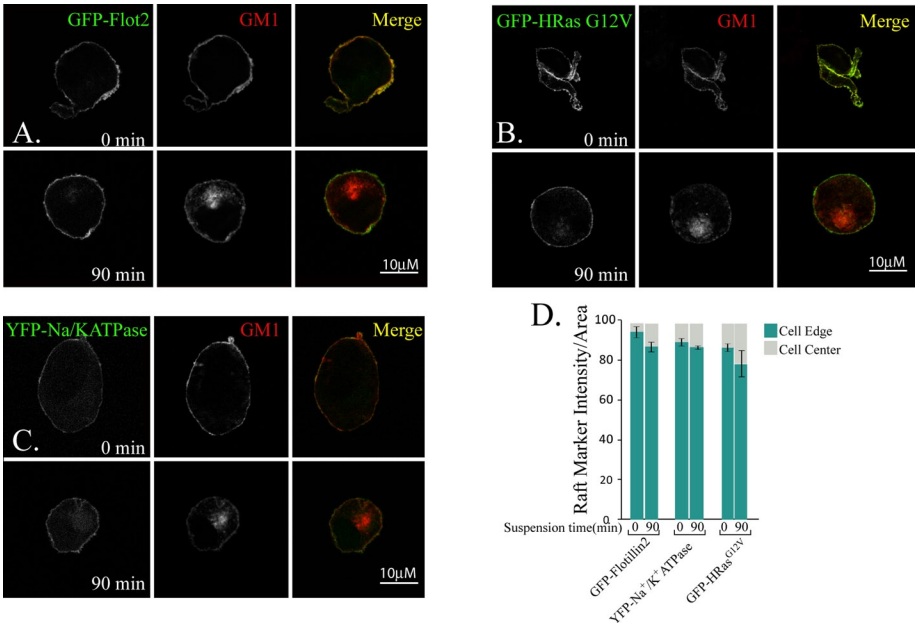

FIGURE 2: Internalization-resistant raft markers. (A–C) Stably adherent NIH 3T3 cells transfected with the indicated GFP or YFP fusions were surface-labeled with CTxB-Alexa 594, detached, and analyzed as in Figure 1. For these markers, most of the protein remained at the cell surface after a 90-min suspension. (D) Fluorescence intensity (as a percentage of total intensity) was determined within the cell edge and the cell center. Values are mean ± SE, n = 15 cells; two independent experiments gave similar results. Bar, 10 μM.

efficiencies. By contrast, flotillin2, connexin43, and Gα_s remained in the PM. When partitioning into raft domains was examined by flotation of detergent extracts on sucrose gradients, most but not all of these proteins shifted from low- to high-density fractions, indicating movement from raft to nonraft domains. All of these events were dependent on expression of Cav1, consistent with the integrin-regulated internalization pathway defined in our previous studies. Flotillin2, connexin43, and H-Ras remained strongly associated with the raft fractions, whereas Gα_s moved entirely into the nonraft fractions. Thus changes in location and changes in raft association are not necessarily coupled.

It is likely that internalization is determined by the association with caveolae. Flotillin is excluded from caveolae (Glebov *et al.*, 2006), consistent with its failure to internalize in suspended cells. Although there are reports that both heterotrimeric G proteins (Oh and Schnitzer, 2001) and connexins (Locke *et al.*, 2005) can associate with caveolin or caveolae, they do not appear to colocalize during detachment-induced endocytosis. By contrast, src family kinases and Ras family GTPases associate with caveolae (Brown and London, 1998; Simons and Toomre, 2000) and are efficiently internalized. The differences in partitioning into ordered versus disordered domains in suspended cells is most likely determined by affinity for cholesterol and other lipid raft components. Proteins such as flotillin2 that have high affinities for cholesterol may remain in ordered domains when cholesterol concentration is lower. By contrast, weakly associated proteins will move to disordered regions after modest decreases in cholesterol content. The behavior reported here is therefore consistent with the known properties of these proteins.

We then chose Gα_s to explore the consequences of these changes in membrane properties for cell signaling. Previous work implicated elevated cAMP and activation of PKA in the termination of anchorage-dependent signaling after cell detachment (Howe and Juliano, 2000). We found that this stimulation depended on the Cav1-dependent internalization of raft constituents. This stimulation was also dependent on the exit of G_s from the lipid rafts because providing a stronger raft targeting sequence prevented both dissociation from the low-density fractions and the increase in cAMP production. Thus, analogous to the reported activation of AC following cholesterol extraction with cyclodextrin (Pontier *et al.*, 2008; Allen *et al.*, 2009), altered domain localization of G_s mediates the increase in cAMP that was implicated in anchorage dependence of growth (Howe and Juliano, 2000).

Here we observed that loss of cell adhesion increased cAMP production even in the absence of receptor agonists. Such behavior is predicted to occur following increased access of active G_s protein for AC (Kukkonen *et al.*, 2001). Increases in the G_s baseline activation due to autocrine stimulation could be responsible for the agonist-independent cAMP elevation after cell detachment. Alternatively, increased membrane fluidity in suspended cells may possibly affect the coupling between G_s and potential regulators such as guanine nucleotide exchange factors (GEFs), GTPase activating proteins (GAPs), and activators of G protein signaling (AGs; Ross and Wilkie, 2000; Blumer *et al.*, 2005; Chan *et al.*, 2011). Overall, an increase in the available pools of active G_s for the AC is most likely responsible for the observed increase in cAMP production following loss of cell adhesion.

Altogether, these data reveal several novel consequences of Cav1-dependent lipid raft internalization following cell detachment. They show that cell adhesion controls the location and activity of multiple signaling and transport proteins through this mechanism, although with unanticipated variations among specific raft markers. They also reveal the mechanism of PKA activation in detached cells. Further analysis will be required to determine how membrane order influences particular signaling pathways (and vice versa) in diverse physiological and pathological contexts such as cell migration and responses to soluble growth factors and cytokines.

MATERIALS AND METHODS

Reagents

Cholera toxin subunit B (CTxB) labeled with Alexa 594 (C22843) was purchased from Molecular Probes (Eugene, OR). Unlabeled CTxB (catalogue no. 227039) and anti–cholera toxin antibody (catalogue no. 227040) were obtained from Calbiochem (San Diego, CA). CTxB was obtained from Sigma (#C8052; St. Louis, MO). Accutase (protease and collagenolytic activity) was obtained from Innovative Cell Technologies (San Diego, CA). Enzyme-Free Cell Dissociation Solution, PBS (phosphate-buffered saline) Based was obtained from Millipore (Billerica, MA). Monoclonal anti–β-tubulin antibody (E7) was obtained from the Developmental Studies Hybridoma Bank (Iowa City, IA). Antibodies against caveolin-1(sc-894), FRS2(sc-8318), H-Ras(sc520), GFP(sc9996), and Gαs (sc823) were obtained from Santa Cruz Biotechnology (Santa Cruz, CA). Anti-Rac1 antibody was obtained from Upstate Biotechnology (Lake Placid, NY). Anti–β1 integrin antibody was a gift from Alan F. Horwitz (University of Virginia, Charlottesville). Anti-PDGFR β(28E1) was obtained from Cell Signaling Technology (Danvers, MA).

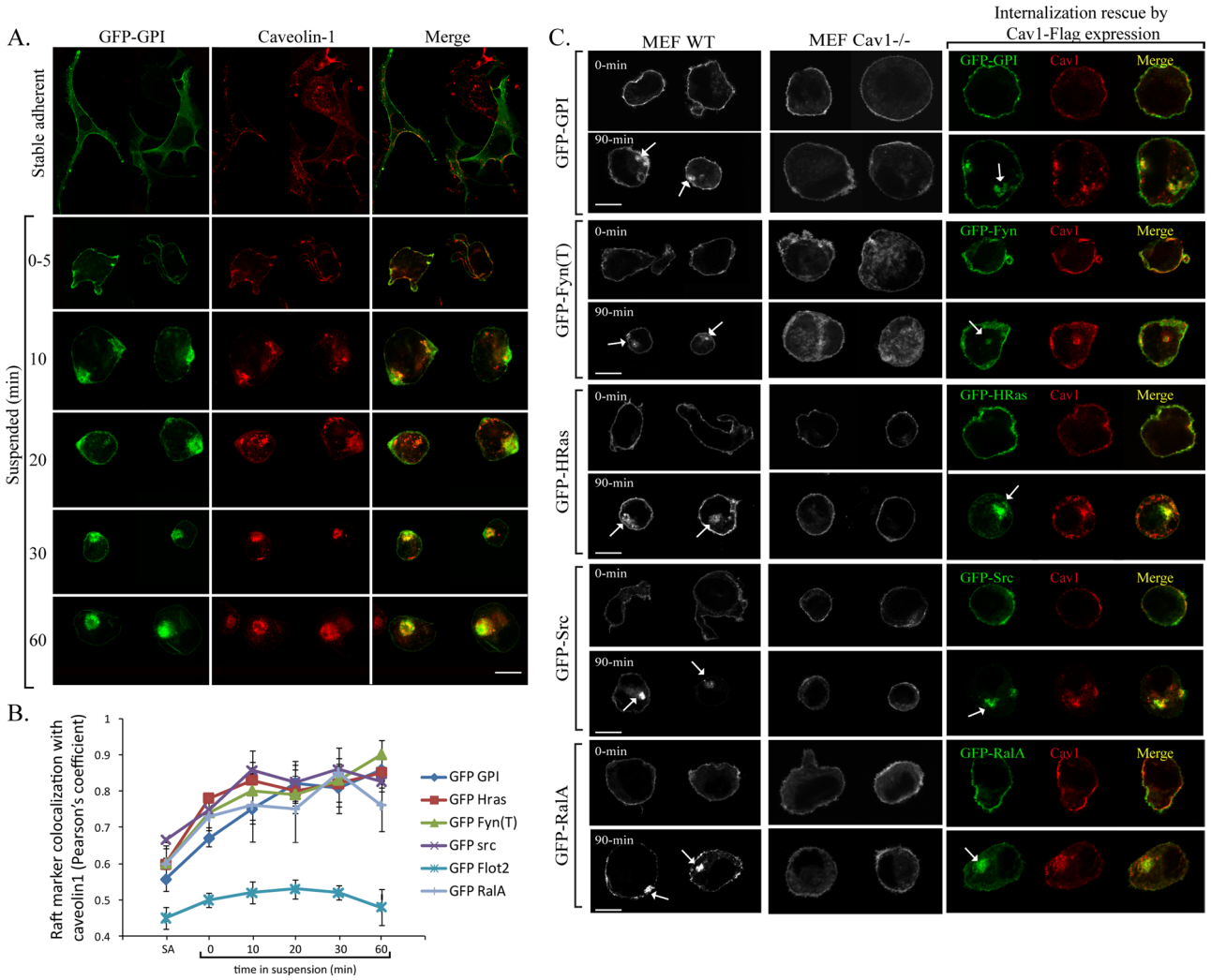

FIGURE 3: Internalization requires caveolin-1. (A) NIH 3T3 fibroblasts transfected with the indicated GFP markers were detached and analyzed as in Figure 1. Cells were then fixed and stained for caveolin-1 in red. Cells expressing GFP–GPI are imaged at the equatorial plane. Images are representative of up to 30 cells at each time point. (B) Pearson's coefficient for colocalization between GFP and Cav1. (C) GFP-tagged constructs were expressed in WT or Cav1$^{-/-}$ MEFs or in Cav1$^{-/-}$ MEFs transfected with Flag-tagged Cav1. These cells were held in suspension, fixed, and analyzed as described earlier in the text. Internalization of GFP-tagged markers was restored in Cav1$^{-/-}$ MEF cells after expression of Cav1. Bar, 10 μM.

Anti-connexin43 was a gift from Brant E. Isakson (University of Virginia). Monoclonal antibodies against RalA(#610221), Fyn(#610164), and flotillin 2 (#610383) were obtained from BD Transduction Laboratories (Franklin Lakes, NJ). An anti-Src antibody was a gift from J. Thomas Parsons (Department of Microbiology, University of Virginia).

Constructs

^{WT}caveolin-1-Flag, RalA-GFP, and ^{WT}Rab11-GFP were as described (del Pozo *et al.*, 2005; Balasubramanian *et al.*, 2007). Flotillin-2–GFP was provided by Ritva Tikkanen (Institute of Biochemistry II, University Clinic of Frankfurt, Germany). The GFP chimera carrying the myristoylation and palmitoylation sequences of Fyn at its N terminus (Fyn(T)-GFP) was described before (Moissoglu *et al.*, 2006). ^{WT}Src-GFP was provided by Michael Weber (University of Virginia, School of Medicine). GPI–GFP was provided by Stephen Lacey (University of Texas–Southwestern Medical Center, Dallas). Gαs-GFP was provided by Mark Rasenick (Department of Physiology and Biophysics [MC 901], College of Medicine, University of Illinois at Chicago). ^{WT}HRas-HA-GFP, ^{G12V}HRas-HA-GFP, and ^{WT}KRas-HA-GFP were provided by John Hancock (Department of Integrative Biology and Pharmacology, The University of Texas Medical School, Houston). Integrin α 5-GFP was provided by Alan F. Horwitz (University of Virginia). The rat α1Na+/K+ ATPase-YFP was provided by Zi-Jian Xie (Department of Physiology and Pharmacology, University of Toledo College of Medicine, Toledo, OH). The Gq/s-GFP was generated by PCR from the pcDNA3 Gαs-GFP (Yu and Rasenick, 2002). The first 10 amino acids of the Gαs were replaced by those of the Gαq by using appropriate primers (primer sense: 5′- CGC GGT ACC ACC ATG ACT CTG GAG TCC ATC ATG GCG TGC TGC GAC CAG CGC AAC GAG GAG AAG -3′). This primer encodes the sequence for Gαq (residues 1→10), which overlaps with the Gαs encoding sequence (starting at position 11). A *Kpn*I restriction site was included before the Gαq initiation codon. The antisense codon incorporated an *Xho*I restriction site (primer antisense: 5′-CGC CTC GAG TTA GAG CAG CTC GTA CTG ACG AAG-3′). Finally, the full-length

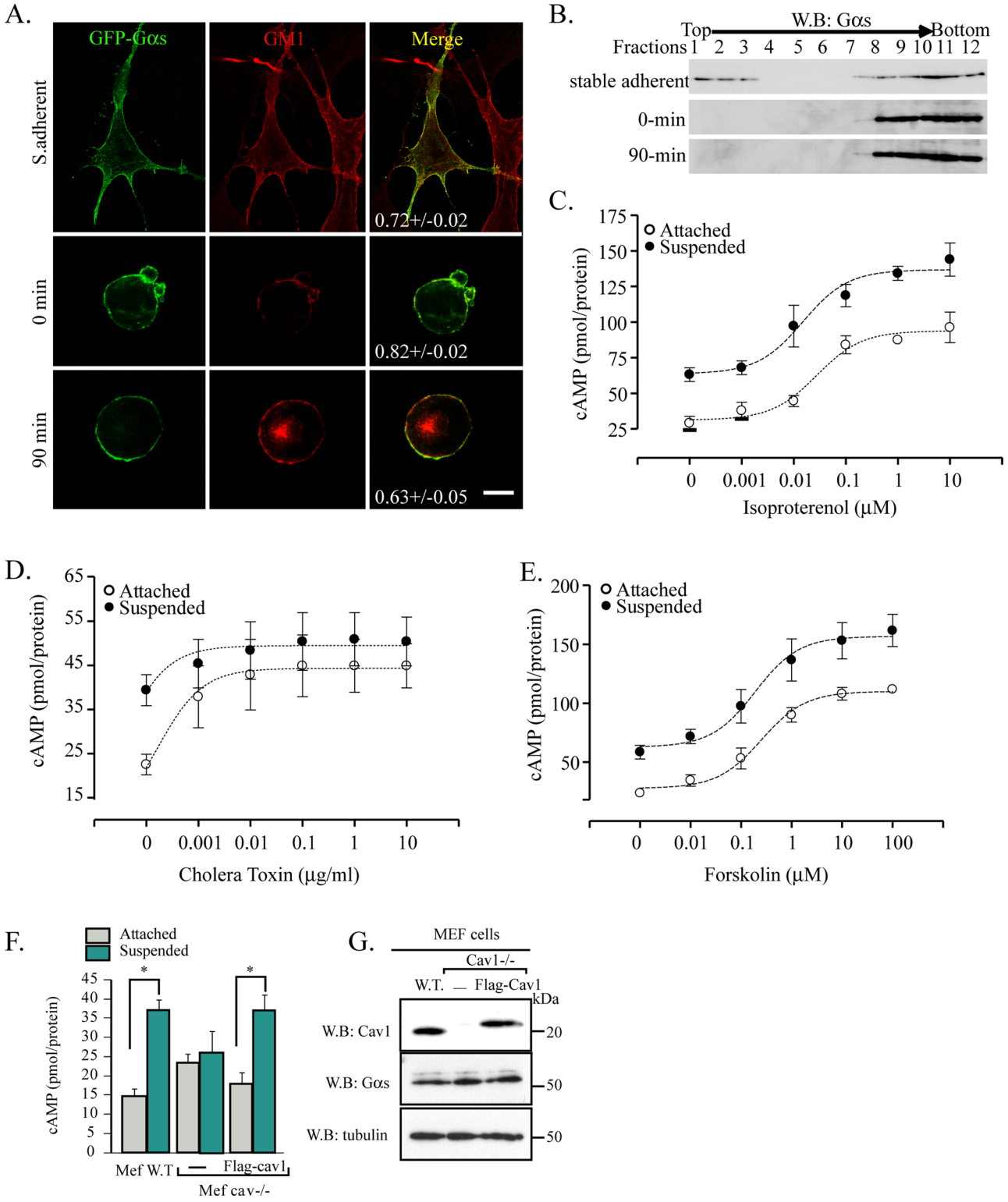

FIGURE 4: Analysis of Gα$_S$. (A) NIH 3T3 cells expressing GFP-G$_s$ were surface labeled with CTxB-Alexa 594, kept adherent or detached, and held in suspension for the indicated times. Numbers in each panel denote Pearson's coefficient determined from 30 cells per condition for each experiment (n = 3). (B) NIH 3T3 cells, either adherent or after detachment, were extracted with Triton X-100 (0.25%), and extracts were separated on sucrose gradients. Fractions were analyzed by immunoblotting for endogenous G$_s$. (C) NIH 3T3 cells were left adherent or detached for 90 min, then stimulated with isoproterenol for 30 min. cAMP was measured as described in *Materials and Methods*. Data are means ± SE, n = 3. (D and E) NIH 3T3 cell fibroblasts were incubated with cholera toxin or forskolin as indicated, then cAMP was assayed in adherent cells or after suspension for 90 min. Data are means ± SE, n = 3. (F) WT, Cav1$^{-/-}$, or Cav1$^{-/-}$ MEFs expressing flag-tagged Cav1 were left adherent or detached for 90 min, then cAMP was assayed. Data are means ± SE, n = 3; two independent experiments gave similar results (*p < 0.05). (G) Total cell extracts from the previous experiment were Western blotted for caveolin-1, G$_s$, and tubulin. Bar, 10 μM.

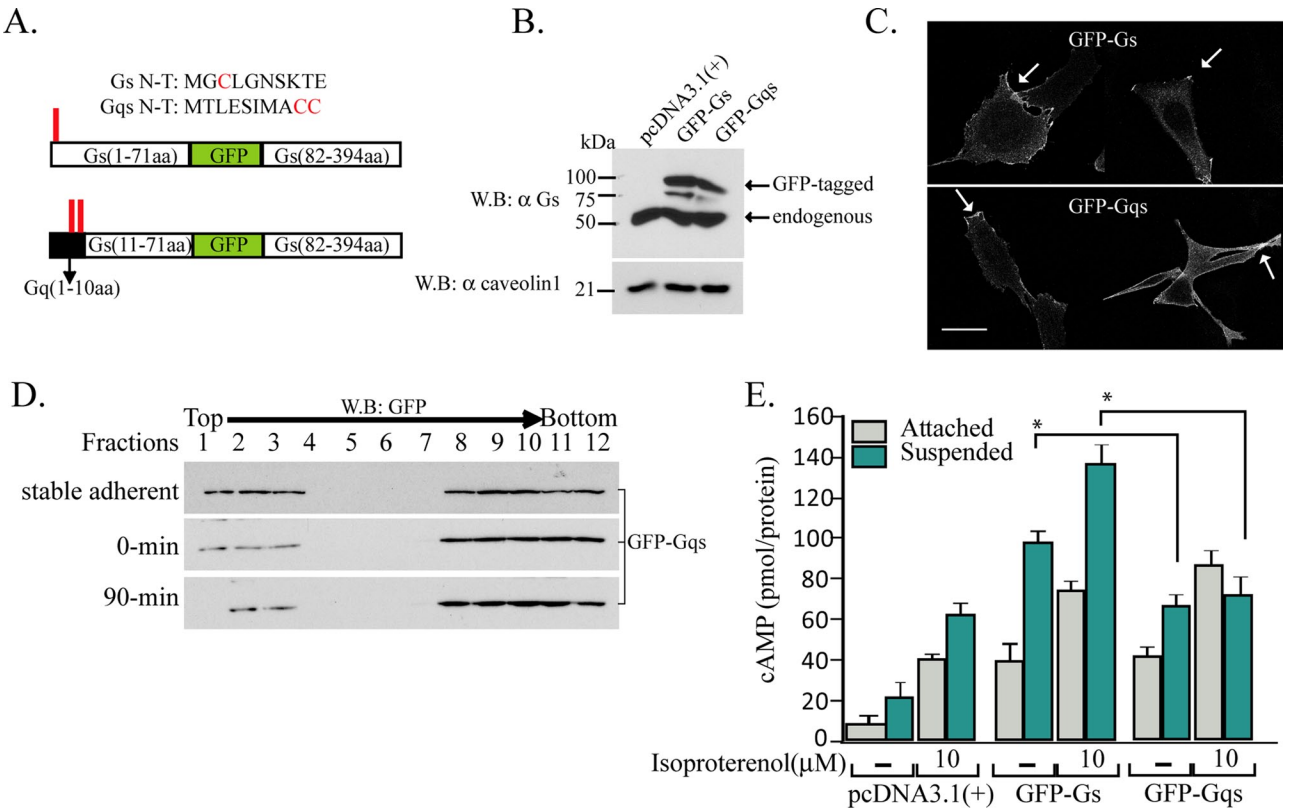

FIGURE 5: Role of the G_s lipid modification. (A) Diagram of WT GFP-G_s and doubly palmitolylated GFP-G_{qs}. Palmitoylation sites are depicted in red. (B) Western blots for G_s- and G_{qs}-GFP show equal expression in NIH 3T3 cells. (C) Localization of G_s- and G_{qs}-GFP. (D) Triton X-100 (0.25%) extracts of cells expressing GFP-G_{qs} were sedimented on sucrose gradients, and fractions were Western blotted for GFP. (E) NIH 3T3 cells were transiently transfected with GFP-G_s, GFP-G_{qs}, or empty pcDNA3.1 vector. Both adherent and 90-min-suspended cells were analyzed for cAMP with and without isoproterenol (10 μM). Data are means ± SE, of two independent experiments, each in triplicate (*$p < 0.05$). Bar, 10 μM.

Gq/s-GFP was cloned in pcDNA3.1(+) at *Kpn*I and *Xho*I sites. The PCR fragments were identified by DNA sequencing.

Tissue culture

MEFs from Cav1$^{-/-}$ and Cav1$^{+/+}$ littermate mice (provided by R. Anderson, University of Texas Health Sciences Center, Dallas) were cultured in DMEM with 10% fetal bovine serum, penicillin, and streptomycin (Invitrogen, Carlsbad, CA). NIH 3T3 fibroblasts were cultivated similarly, but 10% fetal calf serum was used. Cells (5×10^6) were transfected with 40 μg of DNA (10 μg of DNA plasmid plus 30 μg of salmon sperm DNA) by electroporation with the GenePulser Xcell (Bio-Rad Laboratories, Hercules, CA) using 300V and 800 μF. If required, cells were serum-starved for 12 h after electroporation in medium with 0.2% fetal bovine serum. Cells analyzed ~24 h after electroporation generally showed 90–95% transfection efficiency.

For experiments, cells were detached with Accutase, washed, and then held in suspension in DMEM containing 0.5% methylcellulose.

Subcellular fractionation

Light (P17K) and heavy (P100K) membrane fractions were prepared as described previously (del Pozo *et al.*, 2000).

Detergent-resistant membranes

Detergent-resistant membranes (DRMs) were obtained by sucrose flotation after solubilization of whole cells. Briefly, cells were solubilized in ice-cold TNE buffer (25 mM Tris, pH 7.5, 150 mM NaCl, 2 mM EGTA) containing 1 or 0.25% Triton X-100 (vol/vol) (Sigma). NaCl was removed for Gαs solubilization. The homogenate (1 ml) was then adjusted to 40% sucrose by the addition of 1 ml of 80% sucrose prepared in TNE and placed at the bottom of an ultracentrifuge tube. A 5–30% discontinuous sucrose gradient was formed (0.5 ml of 5% sucrose and 2.5 ml of 30% sucrose; both in TNE) and centrifuged at 180,000 × *g* for 16 h. Twelve fractions of 410 μl each were collected from the top of the centrifuge tube. Protein samples were separated in SDS–PAGE, transferred to polyvinylidene difluoride membranes, and incubated with antibodies to detect the presence of the blotted proteins. Immunoblots were digitized in a VISTA-T630 UMax scanner driven by Adobe Photoshop CS (Adobe Systems, Mountain View, CA); quantitative analysis was done with ImageJ software (National Institutes of Health, Bethesda, MD).

cAMP assays

cAMP was assessed with the cAMP Direct Immunoassay Kit, Colorimetric (CalbioChem), according to the manufacturer's recommendations.

Cholera toxin incubations

Stable adherent NIH 3T3 cells were serum-starved for 16 h and then incubated with different concentrations of cholera toxin prepared in DMEM for 1 h at 37°C. Cells were washed with PBS (3X). cAMP was assayed in stable adherent cells or after a 90-min suspension.

Cholesterol depletion

NIH 3T3 cells were rinsed once with PBS and incubated for 1 h at 37°C with increasing concentration of methyl β-cyclodextrin in DMEM. Following depletion treatment, DRMs were prepared and separated on sucrose gradients as described earlier in the text.

Analysis of CTxB distribution in sucrose gradients

Stably adherent cells were placed on ice for 15 min and then incubated with 5 μg/ml unlabeled CTxB (Calbiochem) for 30 min. Cells were washed with cold PBS, kept adherent or detached, and held in suspension during for 0–5 or 90 min. Whole-cell lysates were separated in sucrose gradients to analyze the distribution of GM1 as described earlier in the text. Cell-equivalent amounts of lysates were blotted onto nitrocellulose membranes. Dot blots were incubated with anti-CTxB antibody (1 μg/ml) followed by anti-goat antibody conjugated to horseradish peroxidase, and developed with the ECL+ enhanced chemiluminescence detection system (Amersham, Buckinghamshire, UK). Dot blots were digitized in a VISTA-T630 UMax scanner (UMax, Dallas, TX) and processed as discussed earlier in the text.

Localization of CTxB

Stably adherent cells were placed on ice for 15 min then incubated for 20 min with 2.5 μg/ml CTxB-Alexa 594, as indicated, in PBS. Cells were kept adherent or detached and held in suspension, and the movement of endocytosed CTxB was studied. Labeled cells were fixed in 3.5% paraformaldehyde, mounted in Fluoromount-G (Southern Biotech, Birmingham, AL), observed with a Zeiss LSM 510 laser confocal microscope with a 100X objective (Carl Zeiss, Thornwood, NY), and analyzed with ImageJ software.

Fluorescent image colocalization analysis

Images of cells photographed with the laser confocal microscope at both wavelengths were analyzed with ImageJ software, and the Pearson coefficient was determined with the colocalization threshold plugin (Balasubramanian *et al.*, 2007).

Quantification of raft marker internalization

Fluorescence intensities were calculated as described previously (Balasubramanian *et al.*, 2007).

Statistical significance

Comparisons between data points were done with Student's *t* test (Sigmaplot Statistical Analysis Software, San Jose, CA).

ACKNOWLEDGMENTS

This work was funded by United States Public Health Service grant RO1 GM47214 to M.A.S. A.N. was partially supported by a Postdoctoral Training Fellowship by the General Secretariat of the Organization of American States (OAS), Scholarship Program for Academic Studies.

REFERENCES

Allen JA, Yu JZ, Dave RH, Bhatnagar A, Roth BL, Rasenick MM (2009). Caveolin-1 and lipid microdomains regulate Gs trafficking and attenuate Gs/adenylyl cyclase signaling. Mol Pharmacol 76, 1082–1093.

Alousi AA, Jasper JR, Insel PA, Motulsky HJ (1991). Stoichiometry of receptor-Gs-adenylate cyclase interactions. FASEB J 5, 2300–2303.

Balasubramanian N, Scott DW, Castle JD, Casanova JE, Schwartz MA (2007). Arf6 and microtubules in adhesion-dependent trafficking of lipid rafts. Nat Cell Biol 9, 1381–1391.

Balasubramanian N, Meier JA, Scott DW, Norambuena A, White MA, Schwartz MA (2010). RalA-exocyst complex regulates integrin-dependent membrane raft exocytosis and growth signaling. Curr Biol 20, 75–79.

Beavo JA, Brunton LL (2002). Cyclic nucleotide research—still expanding after half a century. Nat Rev Mol Cell Biol 3, 710–718.

Blumer JB, Cismowski MJ, Sato M, Lanier SM (2005). AGS proteins: receptor-independent activators of G-protein signaling. Trends Pharmacol Sci 26, 470–476.

Bockhorn M, Jain RK, Munn LL (2007). Active versus passive mechanisms in metastasis: do cancer cells crawl into vessels, or are they pushed? Lancet Oncol 8, 444–448.

Brown DA, London E (1998). Functions of lipid rafts in biological membranes. Annu Rev Cell Dev Biol 14, 111–136.

Chan P, Gabay M, Wright FA, Tall GG (2011). Ric-8B Is a GTP-dependent G protein {alpha}s guanine nucleotide exchange factor. J Biol Chem 286, 19932–19942.

De Haan L, Hirst TR (2004). Cholera toxin: a paradigm for multi-functional engagement of cellular mechanisms (Review). Mol Membr Biol 21, 77–92.

del Pozo MA, Alderson NB, Kiosses WB, Chiang HH, Anderson RG, Schwartz MA (2004). Integrins regulate Rac targeting by internalization of membrane domains. Science 303, 839–842.

del Pozo MA, Balasubramanian N, Alderson NB, Kiosses WB, Grande-Garcia A, Anderson RG, Schwartz MA (2005). Phospho-caveolin-1 mediates integrin-regulated membrane domain internalization. Nat Cell Biol 7, 901–908.

del Pozo MA, Price LS, Alderson NB, Ren XD, Schwartz MA (2000). Adhesion to the extracellular matrix regulates the coupling of the small GTPase Rac to its effector PAK. EMBO J 19, 2008–2014.

Gaus K, Le Lay S, Balasubramanian N, Schwartz MA (2006). Integrin-mediated adhesion regulates membrane order. J Cell Biol 174, 725–734.

Glebov OO, Bright NA, Nichols BJ (2006). Flotillin-1 defines a clathrin-independent endocytic pathway in mammalian cells. Nat Cell Biol 8, 46–54.

Howe AK, Juliano RL (2000). Regulation of anchorage-dependent signal transduction by protein kinase A and p21-activated kinase. Nat Cell Biol 2, 593–600.

Kukkonen JP, Nasman J, Akerman KE (2001). Modelling of promiscuous receptor-Gi/Gs-protein coupling and effector response. Trends Pharmacol Sci 22, 616–622.

Lingwood D, Simons K (2010). Lipid rafts as a membrane-organizing principle. Science 327, 46–50.

Locke D, Liu J, Harris AL (2005). Lipid rafts prepared by different methods contain different connexin channels, but gap junctions are not lipid rafts. Biochemistry 44, 13027–13042.

Manes S, Mira E, Gomez-Mouton C, Lacalle RA, Keller P, Labrador JP, Martinez AC (1999). Membrane raft microdomains mediate front-rear polarity in migrating cells. EMBO J 18, 6211–6220.

Marrari Y, Crouthamel M, Irannejad R, Wedegaertner PB (2007). Assembly and trafficking of heterotrimeric G proteins. Biochemistry 46, 7665–7677.

Moissoglu K, Slepchenko BM, Meller N, Horwitz AF, Schwartz MA (2006). In vivo dynamics of Rac-membrane interactions. Mol Biol Cell 17, 2770–2779.

Oh P, Schnitzer JE (2001). Segregation of heterotrimeric G proteins in cell surface microdomainsG(q) binds caveolin to concentrate in caveolae, whereas G(i) and G(s) target lipid rafts by default. Mol Biol Cell 12, 685–698.

Patel HH, Murray F, Insel PA (2008). Caveolae as organizers of pharmacologically relevant signal transduction molecules. Annu Rev Pharmacol Toxicol 48, 359–391.

Pontier SM, Percherancier Y, Galandrin S, Breit A, Gales C, Bouvier M (2008). Cholesterol-dependent separation of the beta2-adrenergic receptor from its partners determines signaling efficacy: insight into nanoscale organization of signal transduction. J Biol Chem 283, 24659–24672.

Ross EM, Wilkie TM (2000). GTPase-activating proteins for heterotrimeric G proteins: regulators of G protein signaling (RGS) and RGS-like proteins. Annu Rev Biochem 69, 795–827.

Schwartz MA (1997). Integrins, oncogenes, and anchorage independence. J Cell Biol 139, 575–578.

Simons K, Toomre D (2000). Lipid rafts and signal transduction. Nat Rev Mol Cell Biol 1, 31–39.

Yu JZ, Rasenick MM (2002). Real-time visualization of a fluorescent G(alpha)(s): dissociation of the activated G protein from plasma membrane. Mol Pharmacol 61, 352–359.